Heliyon 10 (2024) e27653

Contents lists available at ScienceDirect

Heliyon

journal homepage: www.cell.com/heliyon

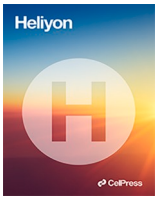

Research article

LncRNA NEAT1 promotes angiogenesis of retinoblastoma cells through regulation of the miR-106a/HIF-1α axis

Ying Liu [a], Zhiyuan Xin [b], Kun Zhang [a], Xin Jin [b], Dajiang Wang [b,*]

[a] Department of Ophthalmology, Beijing Rehabilitation Hospital, Capital Medical University, Beijing 100144, China
[b] Department of Ophthalmology, Senior Department of Ophthalmology, The Third Medical Center of PLA General Hospital, Beijing 100144, China

ARTICLE INFO

Keywords:
Retinoblastoma
Angiogenesis
lncRNA NEAT1
miR-106a
HIF-1α

ABSTRACT

Objective: To explore the role and mechanisms of lncRNA nuclear enriched abundant transcript 1 (NEAT1) in angiogenesis of retinoblastoma (RB) cells.
Methods: This study investigated the roles of NEAT1 in RB progression. The RNA expression levels of NEAT1, miR-106a, and hypoxia-inducible factor-1alpha (HIF-1α) examined by quantitative reverse transcription polymerase chain reaction (RT-qPCR) were compared between RB cells and normal retinal pigment epithelial (RPE) cells. The binding sites between NEAT1 and miR-106a, and between miR-106a and HIF-1α were predicted by the TargetScan database and verified using the dual-luciferase reporter assay. By transfection of overexpression plasmid or shRNA of NEAT1, and/or treatment of miR-106a inhibitor or mimics, proliferation, invasion, and angiogenesis of RB cells (measured by the MTT assay, the Transwell assay, and the tube formation assay, respectively) were compared between groups. Group comparisons were analyzed using one-way analysis of variance (ANOVA), and Tukey's post-hoc test was employed for further statistical assessment. P-value less than 0.05 was considered statistically significant.
Results: The RNA expression levels of NEAT1 and HIF-1α were upregulated in RB cells, whereas the expression level of miR-106a was downregulated compared with RPE cells. NEAT1 overexpression or miR-106a knockdown advanced proliferation, invasion, and tube formation of RB cells. As a target of NEAT1, miR-106a could sponge HIF-1α to downregulate HIF-1α expression level. Functional analyses indicated that miR-106a knockdown reversed the inhibitory effects of NEAT1 silencing on the proliferation, invasion, and tube formation of RB cells. Furthermore, miR-106a overexpression suppressed RB cell angiogenesis by downregulating HIF-1α expression level.
Conclusion: NEAT1 promoted proliferation, invasion, and angiogenesis of RB cells through upregulation of HIF-1α expression level by sponging miR-106a, demonstrating that NEAT1 may be a novel target for RB treatment.

1. Introduction

Retinoblastoma (RB) is a prevalent type of eye cancer primarily affecting young children, constituting 4% of all childhood eye tumors [1,2]. Despite advancements in novel treatments and pharmacological interventions, RB mortality remains elevated, mainly necessitating eyeball removal to impede tumor progression [3,4]. The current therapeutic approaches involve chemotherapy, surgery,

* Corresponding author. Ph.D. Department of ophthalmology, Senior Department of Ophthalmology, the Third Medical Center of PLA General Hospital, 69 Yongding Road, Haidian District, Beijing 100089, China.
E-mail address: wangdajiang1688@163.com (D. Wang).

https://doi.org/10.1016/j.heliyon.2024.e27653
Received 17 September 2023; Received in revised form 26 February 2024; Accepted 5 March 2024
Available online 9 March 2024

and external beam radiotherapy, and these treatments are associated with adverse effects, such as the risk of secondary malignancies. Hence, there is a critical need to identify further effective therapeutic strategies for RB.

Long non-coding RNAs (lncRNAs), a class of RNAs exceeding 200 nucleotides without annotated coding regions, play pivotal roles in regulating various cellular processes, including differentiation, proliferation, migration, invasion, and apoptosis [5,6]. Recent evidence has revealed that several lncRNAs can regulate RB progression [7,8]. For instance, lncRNA KCNQ1OT1 has been implicated in promoting cancer progression by regulating RB cell proliferation and migration through downregulation of miR-134 [9]. Another lncRNA, nuclear enriched abundant transcript 1 (NEAT1), has been identified as an oncogenic gene in numerous human cancer types, with dysregulation tightly linked to cancer carcinogenesis and progression [10–12]. Recent findings indicated the elevated NEAT1 expression in RB tissues and cells compared with normal controls [13]. Moreover, NEAT1 appears to exacerbate RB progression through interacting with the miR-204/CXCR4 axis or the miR-24-3p/LRG1 axis [13–15]. However, the exact function and specific mechanisms of NEAT1 in RB remain to be investigated.

MicroRNAs (miRNAs), small non-coding RNAs spanning 18–22 nucleotides, play crucial roles in the onset and advancement of various diseases, encompassing cancers, cardiovascular diseases, and glioblastoma [16,17]. Recent investigations have indicated a diminished expression of miR-106a in several cancer types, including prostate cancer and breast cancer, suggesting its potential as a biomarker [18,19]. In addition to its potential as a promising biomarker for several forms of cancer, miRNA-106a (miR-106a) could also regulate cancer cells proliferation, apoptosis, migration, and metastasis through different signaling pathways. Previous studies that support this hypothesis have shown that miRNA-106a promoted the migration and proliferation of breast cancer cells by binding to DAX-1 [19]. Additionally, miR-106a promoted prostate carcinoma cell growth by downregulating phosphatase tension homolog expression [20]. However, the exact function and mechanisms of miR-106a in RB have not yet been well elucidated.

Hypoxia-inducible factor-1alpha (HIF-1α), a vital molecular regulator in hypoxia signaling, plays a crucial role in restoring oxygen homeostasis by mediating glycolysis, erythropoiesis, and angiogenesis [21]. Its involvement in cancer progression is marked by the modulation of hypoxia-responsive gene expression, influencing cell proliferation, energy metabolism, invasion, and metastasis [21–23]. Notably, studies have recently demonstrated that HIF-1α was upregulated in RB tissues [9,24]. Moreover, HIF-1α level was closely related to the survival and proliferation of RB cells [25,26]. Besides, HIF-1α has been implicated in vascular development and angiogenesis [27–29]. Given the importance of angiogenesis in the stroma for cancer progression, this bioinformatic analysis predicted binding sites between miR-106a and HIF-1α. The objective of the present study was to investigate whether miR-106a could regulate key biological processes in RB cells, including proliferation, invasion, and angiogenesis, through interacting with HIF-1α.

In the present study, the roles and underlying mechanisms of NEAT1 in RB were explored. The expression level of NEAT1 was upregulated in RB cells. Gain- and loss-of-function experiments revealed that NEAT1 promoted the proliferation, invasion, and angiogenesis of RB cells via the miR-106a/HIF-1α axis, thereby aggravating the progression of RB. This study aimed to address the gaps in existing knowledge and prior research by emphasizing several key strengths. One of the primary strengths lies in the exploration of lncRNAs, specifically concentrating on NEAT1. While previous studies have implicated various lncRNAs in RB progression [7,8], the present study uniquely assessed the regulatory role of NEAT1, shedding light on its potential as a therapeutic target. Moreover, the integration of miR-106a and its interplay with HIF-1α could add another layer of complexity to our understanding of RB pathogenesis. Although miRNAs have been implicated in various cancer types [16,17], the specific functions of miR-106a in RB remain elusive. By investigating its regulatory role in conjunction with HIF-1α, this study pioneered a comprehensive exploration of their involvement in RB progression. Additionally, this study employed a robust methodology, including cell culture experiments, molecular analyses, and functional assays. Consequently, this study distinguished itself by elucidating the intricate roles of NEAT1, miR-106a, and HIF-1α in RB, providing a unique perspective on potential therapeutic targets.

2. Materials and methods

Ethical approval

The current study was approved by the Ethics Committee of Beijing Rehabilitation Hospital (Beijing, China; Approval No. 2019bkkyLW007).

2.1. Cell culture

Normal retinal pigment epithelial cells (ARPE-19) and RB cells (Y-79, SO-RB50, and HXO-RB44) were provided by the American Type Culture Collection (ATCC; Manassas, VA, USA). The cells were cultured in a Dulbecco's modified Eagle's medium (DMEM) (Gibco, New York, NY, USA), which was supplemented with 10% fetal bovine serum (FBS) and 1% penicillin-streptomycin (PenStrep) (Grand Island, NY, USA). The cells were cultured in a humidified incubator (37 °C, 5% CO_2) and the media were changed every 2 days. Cells were cultured until passage 3, and they were then utilized for subsequent experiments.

2.2. Cell transfection

The lentiviruses used in this study, including sh-NEAT1, sh-NC, pcDNA3.1 overexpression lentivirus (pc-NEAT1 and pc-HIF-1α), and corresponding negative controls (pc-DNA3.1, pc-NC), as well as miR-106a mimics, mimics' control, miR-106a inhibitor, and the inhibitor control, were supplied by GenePharm (Shanghai, China). Y-79 cells (1×10^4 cells/well) were seeded into 24-well plates and grown until reaching the confluence of 70%. The confluent cells were subsequently transfected with RNAs (10 nM) or vectors (1 μg per

well) using the Invitrogen Lipofectamine 3000 reagent (Thermo Fisher Scientific, Inc., Waltham, MA, USA). The sequences used for cell transfection were summarized as follows:

sh-NEAT1: 5′-GGGAGAGATGACTGAGTTA-3’;
sh-NC: 5′-TTCTCCGAACGTGTCACGT-3’;
miR-106a mimics: 5′-AAAAGUGCUUACAGUGCAGGUAG-3’;
miR-106a mimics’ control: 5′-UUCUCCGAACGUGUCACGUTT-3’;
miR-106a inhibitor: 5′-CUACCUGCACUGUAAGCACUUUU-3’;
miR-106a inhibitor control: 5′-CAGUACUUUUGUGUAGUACAA-3’.

2.3. Quantitative reverse transcription polymerase chain reaction (RT-qPCR)

Total RNA was isolated using TRIzol® reagent (Invitrogen, Carlsbad, CA, USA). In addition, cDNA was synthesized using the PrimeScript RT Master Mix (Takara, Shiga, Japan), and RT-qPCR was conducted on a Real-Time PCR system (7500; Thermo Fisher Scientific, Inc.) using TB Green Fast qPCR Mix (Takara). The thermal cycling conditions for PCR were as follows: initial denaturation at 94 °C for 6 min, followed by 35 cycles of denaturation at 92 °C for 35 s, annealing at 58 °C for 35 s, extension at 70 °C for 35 s, and a final extension at 70 °C for 10 min. The $2^{-\Delta\Delta CT}$ method was used to quantify the levels of genes. The primer sequences used in this study were listed as follows:

NEAT1-F: 5′-CTTCCTCCCTTTAACTTATCCATTCAC-3′;
NEAT1-R: 5′-CTCTTCCTCCACCATTACCAACAATAC-3′;
MiR-106a-F: 5′-GAAAAGTGCTTACAGTGCAG-3′;
MiR-106a-R: 5′-GTCCAGTTTTTTTTTTTTTTTCTACCT-3′;
HIF-1α-F: 5′-TGATTGCATCTCCATCTCCTACC-3′;
HIF-1α-R: 5′-GACTCAAAGCGACAGATAACACG-3′;
GADPH-F: 5′-TGGTGAAGACGCCAGTGGA-3′;
GAPDH-R: 5′-GCACCGTCAAGGCTGAGAAC-3′;
U6 small nuclear RNA-F: 5'-CTCGCTTCGGCAGCACA-3';
U6 small nuclear RNA-R: 5'-AACGCTTCACGAATTTGCGT-3'.

2.4. Western blotting

Total protein was collected using the RIPA kit (#P0027; Beyotime, Shanghai, China). A BCA kit (#23229; Thermo Fisher Scientific, Inc.) was utilized to measure protein concentrations. A total of 10 μg protein was electrophoresed through 10% sodium dodecyl-sulfate polyacrylamide gel electrophoresis (SDS-PAGE) and transferred onto polyvinylidene difluoride (PVDF) membranes (#3010040001; Millipore, Burlington, MA, USA). The membranes were blocked with 5% milk for 2 h at room temperature (RT) and incubated overnight with primary antibodies against HIF-1α (#ab179483; 1:2000; Abcam, Cambridge, UK), VEGF (#ab150375; 1:4000; Abcam), Ki-67 (#ab16667; 1:1000; Abcam), MMP9 (#ab76003; 1:5000; Abcam), and GAPDH (#ab181602; 1:10,000; Abcam) at 4 °C. The membranes were washed four times, and the appropriate secondary horseradish peroxidase (HRP) antibodies (1:5000) were added. The membranes were subsequently incubated for 2 h at RT. After incubation, the membranes were washed four times with TBST. The protein bands were detected using enhanced chemiluminescence with a CL-XPosure™ film (Thermo Fisher Scientific). Band intensities were quantified using ImageJ 1.50 software.

3. MTT assay

Y79 cells (3×10^4 cells/well) were seeded into 96-well plates for 48 h. 15 μL MTT solution (5 mg/mL; Sigma-Aldrich, St. Louis, MO, USA) was added to the plates. The plates were subsequently incubated at RT for 5 h. The media were removed and 200 μL DMSO was added to plates, followed by incubation for 15 min. To evaluate cell viability, the optical density (OD) value at 570 nm was measured using a spectrophotometer (BD Biosciences, Franklin Lakes, NJ, USA).

3.1. Transwell assay

Cell invasion was examined using the Transwell assay as previously described [30]. In brief, Y-79 cells (1×10^5 cells/well) were added to the upper chamber of the Transwell insert (8 μm pore size; BD Biosciences) with a serum-free medium. A DMEM supplemented with 10% FBS was added to the lower chamber. After 24 h, cells that were migrated into the lower chamber were fixed with 4% paraformaldehyde and incubated with 0.1% crystal violet for 30 min at RT. After washing, the cells were counted under an inverted microscope (Nikon, Tokyo, Japan) from five randomly selected fields.

3.2. Tube formation assay

150 μL thawed Matrigel solution (10 mg/mL, BD Biosciences) was added to each well of a 48-well plate and was incubated at RT for 30 min. After cultivation in a DMEM (serum starvation) for 2 h, the Y-79 cells were seeded into the 48-well plates and were incubated at RT for 5 h. Tube formation was detected by phase-contrast microscopy (Nikon), and the total number of tubes was quantified by

ImageJ 1.50 software.

3.3. Luciferase reporter assay

Wild-type (WT) NEAT1, mutant (MUT) NEAT1, WT HIF-1α, and MUT HIF-1α fragments were purchased from GenePharma and inserted into PsiCHECK-2 vectors (Promega, Madison, WI, USA). For the dual-luciferase reporter assay, Y-79 cells (5×10^4 cells/well) were seeded into 24-well plates and cultured to reach a confluence of 70%. The cells were subsequently co-transfected for 48 h with NEAT1-WT, NEAT1-MUT, HIF-1α-WT, HIF-1α-MUT, and either miR-106a mimics or mimics' control using Lipofectamine® 3000 reagent (Invitrogen). Luciferase activity was detected using the Dual-Luciferase Assay system (Promega).

3.4. Statistical analysis

All data were analyzed using SigmaStat 10.0 software (SPSS) and presented as mean ± standard deviation (SD). The normality test was conducted on the data using the Kolmogorov-Smirnov test. Group comparisons were analyzed using one-way analysis of variance (ANOVA), and Tukey's post-hoc test was employed for further statistical assessment. $P < 0.05$ was considered statistically significant.

4. Results

4.1. NEAT1, miR-106a, and HIF-1α expression levels were dysregulated in RB cells

To explore whether NEAT1, miR-106a, and HIF-1α expression levels would be dysregulated in RB cells, these expression levels in normal retinal pigment epithelial cells (ARPE-19) and RB cells (Y-79, SO-RB50, and HXO-RB44) were measured by RT-qPCR. The mRNA levels of NEAT1 and HIF-1α were significantly higher ($P < 0.05$), while miR-106a mRNA level was significantly lower ($P < 0.05$), in RB cells relative to ARPE-19 cells (Fig. 1A–**C**). Furthermore, the protein levels of HIF-1α and VEGF were higher in RB cells than those in ARPE-19 cells as measured by Western blotting (Fig. 1D). Taken together, the expression levels of NEAT1, miR-106a, and HIF-1α were dysregulated during RB, and they might play key roles in disease progression.

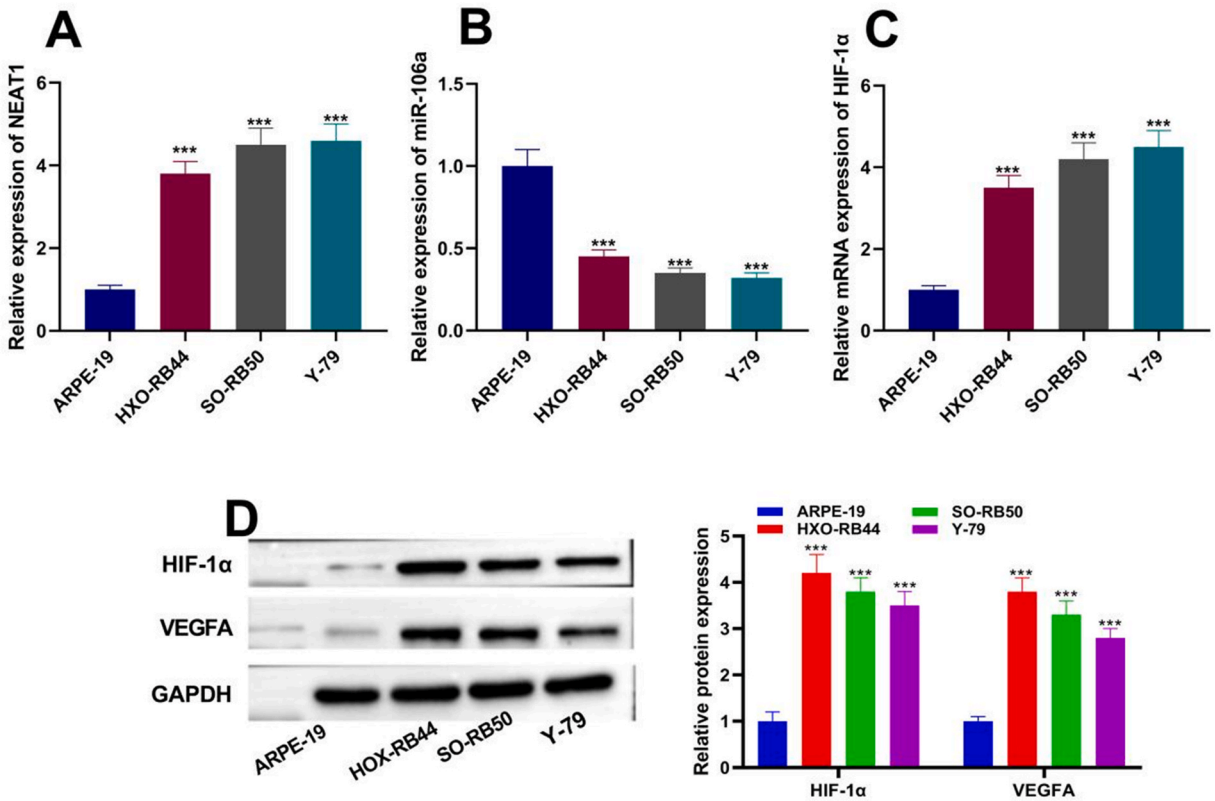

Fig. 1. Expression levels of NEAT1, miR-106a, and HIF-1α in RB cells. The mRNA levels of (A) NEAT1, (B) miR-106a and HIF-1α, and (C) ARPE-19 in RB cells (Y-79, SO-RB50, and HXO-RB44) were measured by RT-qPCR. (D) The protein levels of HIF-1α and VEGF in these cells were measured by Western blotting (uncropped blot is available in Supplementary Fig. 1D-GAPDH, Fig. S1D-HIF-1A, and Fig. S1D-VEGFA).

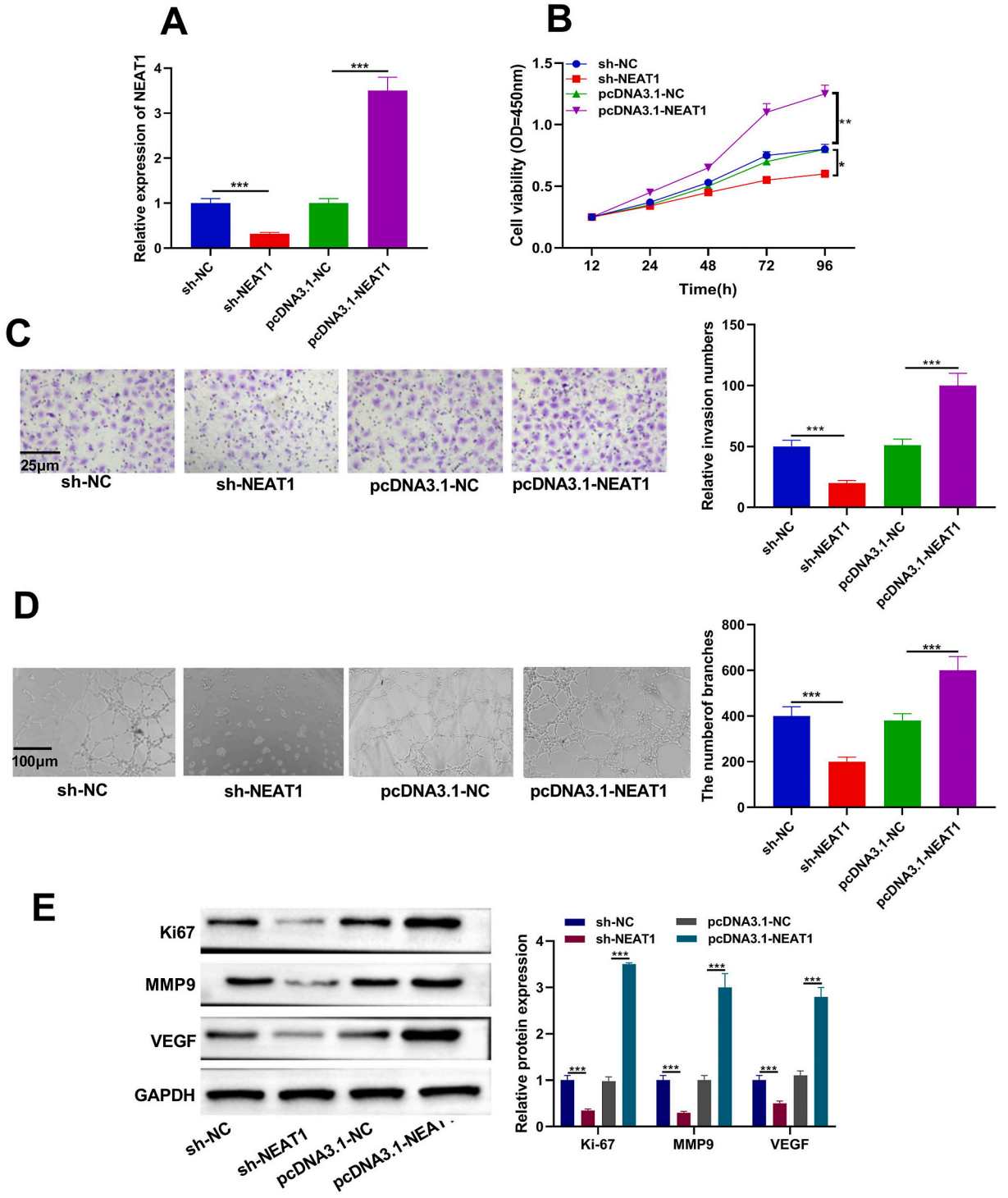

Fig. 2. NEAT1 knockdown inhibits the proliferation, invasion, and tube formation of RB cells. Y-79 cells were transfected with sh-NC, sh-NEAT1, pc-DNA3.1, or pc-NEAT1. (A) The expression level of NEAT1 was measured by RT-qPCR. (B) Y-79 cell proliferation was measured using the MTT assay. (C) The invasion of pretreated Y-79 cells was assessed by the Transwell assay (magnification = 100×). (D) The capillary-like structure formation of pretreated Y-79 cells was evaluated by tube formation assay (magnification = 100×). (E) Ki-67, MMP9, and VEGF protein levels in Y-79 cells were detected by Western blotting ((uncropped blot is available in supplementary Fig.2E-GAPDH, Fig.2E-KI67, Fig.2E-MMP9, and Fig.2E-VEGF).

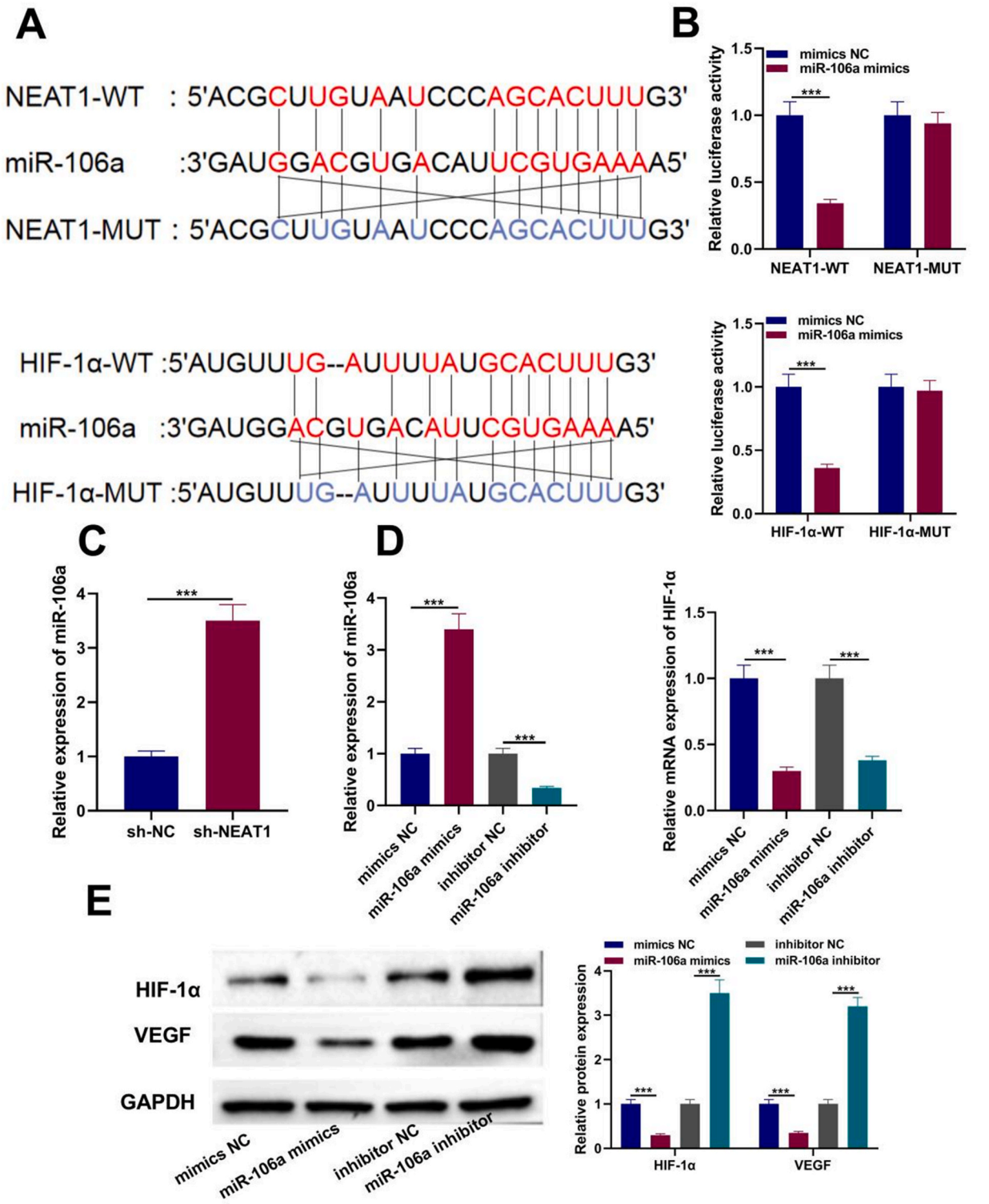

(caption on next page)

Fig. 3. The targeting relationship between NEAT1, HIF-1α, and miR-106a. (A) The potential binding sites between HIF-1α and miR-106a, NEAT1, and miR-106a were predicted using the TargetScan database. (B) Luc-NEAT1-WT or Luc-NEAT1-MUT plasmids were co-transfected with miR-106a mimics or NC mimics in Y-79 cells for 24 h, followed by luciferase quantification (top), and Luc-HIF-1α-WT or Luc-HIF-1α-MUT plasmids were co-transfected with miR-106a mimics or NC mimics in Y-79 cells for 24 h, followed by luciferase quantification (bottom). (C) Y-79 cells were transfected with sh-NC or sh-NEAT1 for 24 h and miR-106a levels were subsequently detected by RT-qPCR. (D) Y-79 cells were transfected with miR-106a mimics, NC mimics, miR-106a inhibitor, or the NC inhibitor for 24 h, and the levels of miR-106a (left) and HIF-1α (right) were detected by RT-qPCR. (E) Y-79 cells were transfected with miR-106a mimics, NC mimics, miR-106a inhibitor, or the NC inhibitor for 24 h, and HIF-1α and VEGF protein levels were subsequently detected by Western blotting (uncropped blot is available in supplementary Fig.3E-GAPDH, Fig.3E-HIF1A, and Fig.3E-VEGF).

4.2. NEAT1 promoted the proliferation, invasion, and angiogenesis of RB cells

To clarify the potential roles of NEAT1 in RB, Y-79 cells were transfected with sh-NC, sh-NEAT1, pc-DNA3.1, or pc-NEAT1. The efficacy of transfection was determined by RT-qPCR. NEAT1 expression level in Y-79 cells was significantly downregulated after transfection with sh-NEAT1 ($P < 0.05$), while it was upregulated after transfection with pc-NEAT1 relative to the negative control group (Fig. 2A). The results of MTT assay revealed that NEAT1 knockdown markedly suppressed cell proliferation, while NEAT1 overexpression promoted cell proliferation ($P < 0.05$) (Fig. 2B). Furthermore, the results of the Transwell assay indicated that the Y-79 cell invasion was inhibited after transfection with sh-NEAT1, while it was promoted after transfection with pc-NEAT1 (Fig. 2C). To further assess the role of NEAT1 in angiogenesis, the tube formation assay was conducted. NEAT1 knockdown significantly inhibited tube formation ($P < 0.05$). In contrast, NEAT1 overexpression promoted tube formation (Fig. 2D). Moreover, the expression levels of Ki-67, MMP9, and VEGF were reduced in Y-79 cells transfected with sh-NEAT1, whereas those of the same genes were upregulated in Y-79 cells transfected with pc-NEAT1 ($P > 0.05$) (Fig. 2E). Taken together, NEAT1 could promote RB cell proliferation, invasion, and angiogenesis.

4.3. The correlation between NEAT1, miR-106a, and HIF-1α in RB cells

Generally, lncRNAs may function as molecular sponges for miRNAs. According to the dysregulation of NEAT1, miR-106a, and HIF-1α in RB cells, it was hypothesized that there might be biological associations between NEAT1, miR-106a, and HIF-1α. Bioinformatic analysis predicted the presence of complementary sites between NEAT1 and miR-106a, and between miR-106a and HIF-1α (Fig. 3A). Furthermore, the results of the dual-luciferase reporter assay disclosed that the luciferase activity in NEAT1-WT was inhibited by miR-106a mimics, while luciferase activity was not altered in the NEAT1-MUT group (Fig. 3B). Additionally, the luciferase activity in the HIF-1α-WT group was significantly reduced by the miR-106a mimic ($P < 0.05$). No significant change was found in the HIF-1α-MUT group ($P > 0.05$) (Fig. 3B). NEAT1 knockdown reduced the miR-106a expression level (Fig. 3C). The miR-106a expression level was elevated in Y-79 cells transfected with miR-106a mimics, whereas it was reduced in Y-79 cells transfected with the miR-106a inhibitor. Collectively, these findings confirmed successful transfection. Moreover, HIF-1α expression level in Y-79 cells was significantly upregulated by transfection with the miR-106a inhibitor ($P < 0.05$), while it was reduced by transfection with the miR-106a mimics (Fig. 3D). Consequently, these data indicated that NEAT1 could negatively regulate miR-106a expression level, and miR-106a could negatively regulate HIF-1α expression level.

Knockdown of miR-106a reversed the inhibitory effects of sh-NEAT1 on proliferation, invasion, and angiogenesis of RB cells.

To further explore whether NEAT1 could modulate RB cell progression by targeting miR-106a, Y-79 cells were transfected with miR-106a inhibitor, NC inhibitor, sh-NEAT1 + NC inhibitor, or sh-NEAT1 + miR-106a inhibitor. Cell proliferation was enhanced in the Y-79 cells transfected with miR-106a inhibitor ($P < 0.05$), and it was reduced by silencing of NEAT1. Additionally, the reduction of cell proliferation was reversed following miR-106a knockdown (Fig. 4A). The results of the Transwell and tube formation assays revealed that miR-106a knockdown significantly promoted Y-79 cell invasion and tube formation ($P < 0.05$) (Fig. 4B and **C**). Meanwhile, the suppression of invasion and tube formation induced by NEAT1 knockdown was also significantly reversed by miR-106a inhibitor ($P < 0.05$) (Fig. 4B and **C**). Furthermore, miR-106a knockdown increased Ki-67, MMP9, and VEGF protein levels in Y-79 cells. Consistently, the miR-106a inhibitor partly abolished the suppressive effect of sh-NEAT1 on Ki-67, MMP9, and VEGF expression levels (Fig. 4D). Taken together, these data indicated that NEAT1 could positively regulate RB cell proliferation, invasion, and tube formation by acting as a molecular sponge for miR-106a.

4.4. NEAT1 regulated RB cell proliferation, invasion, and angiogenesis through the miR-106a/HIF-1α axis

To further examine how NEAT1 could promote RB progression through the miR106a/HIF-1α axis, pc-HIF-1α, pc-HIF-1α + miR-106a mimics, pc-HIF-1α + sh-NEAT1, or their negative controls were transfected into Y-79 cells. Firstly, RT-qPCR and Western blotting were performed to measure the transfection efficiency of pc-HIF-1α. The mRNA and protein levels of HIF-1α were both markedly upregulated in the pc-HIF-1α group compared with those in the pc-NC group ($P < 0.05$) (Fig. 5A and **B**). The MTT assay data indicated that cell proliferation was enhanced after pc-HIF-1α transfection, whereas the proliferative effect was blocked by miR-106a overexpression or NEAT1 knockdown (Fig. 5C). Additionally, HIF-1α overexpression significantly increased Y-79 cell invasion and angiogenesis ($P < 0.05$); however, these effects were suppressed when the cells were co-transfected with miR-106a mimics or sh-NEAT1 (Fig. 5D and **E**). Furthermore, the protein levels of Ki-67, MMP9, and VEGF were upregulated in Y-79 cells transfected with pc-HIF-1α. NEAT1 knockdown or miR-106a overexpression inhibited the increased expression levels of Ki-67, MMP9, and VEGF

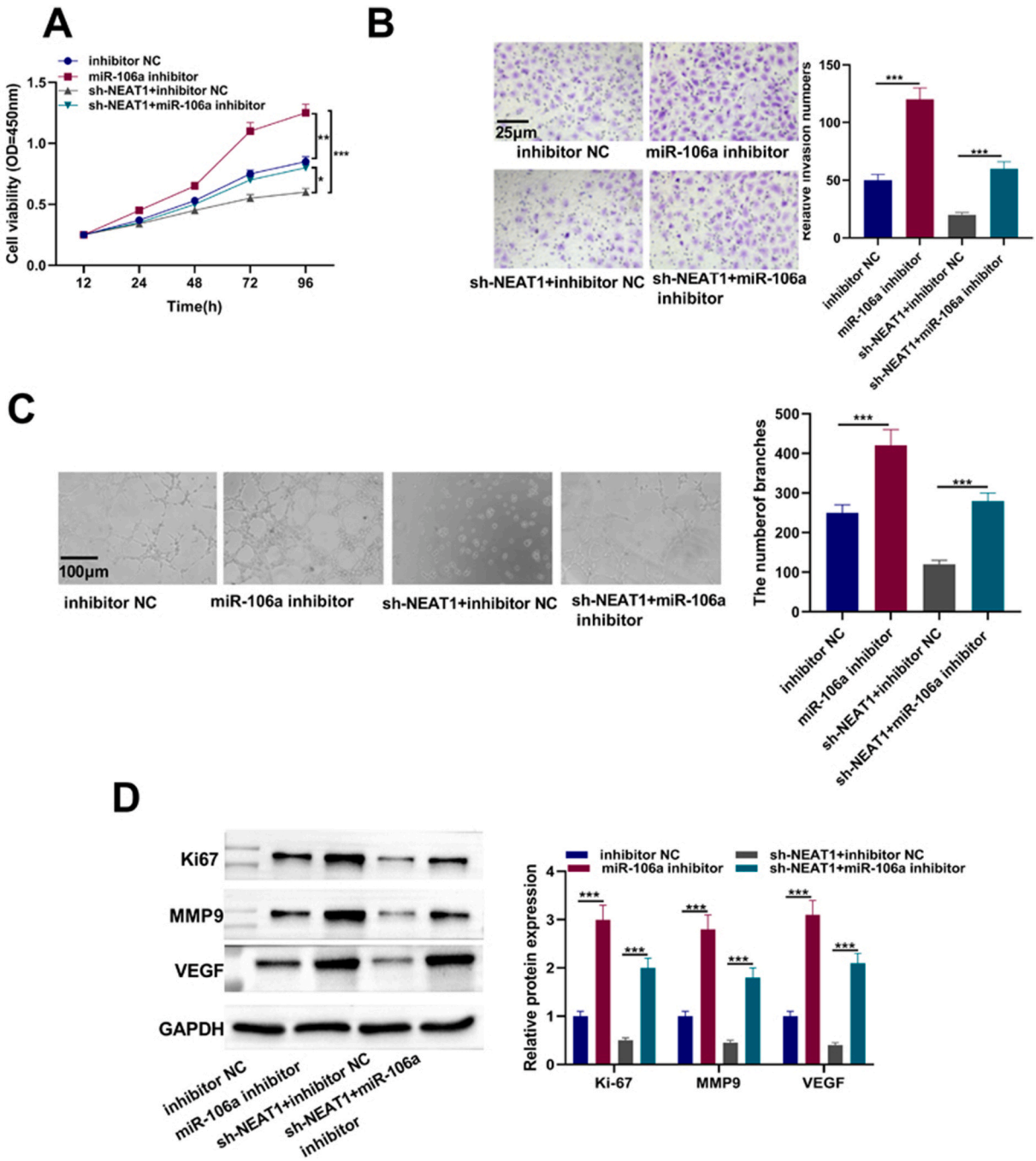

Fig. 4. MiR-106a knockdown reverses the effects of sh-NEAT1 on RB cells. Y-79 cells were transfected with NC inhibitor or miR-106a inhibitor, or co-transfected with sh-NEAT1 and the NC inhibitor, sh-NEAT1, and miR-106a inhibitor. (A) Cell proliferation was assessed by the MTT assay. (B) The Transwell assay was employed to evaluate the invasion of pretreated Y-79 cells (magnification = 100×). (C) The capillary-like structure formation of pretreated Y-79 cells was assessed using the tube formation assay (magnification = 100×). (D) Ki-67, MMP9, and VEGF protein levels were detected by Western blotting (uncropped blot is available in supplementary Fig.4D-GAPDH, Fig.4D-KI67, Fig.4D-MMP9, and Fig.4D-VEGF).

induced by pc-HIF-1α ($P < 0.05$) (Fig. 5F). Collectively, these findings demonstrated that NEAT1 could regulate cell proliferation, invasion, and angiogenesis through the miR-106a/HIF-1α signaling pathway. Fig. 6 illustrates the mechanism of NEAT1, miR-106a/HIF-1α in RB versus normal RPE.

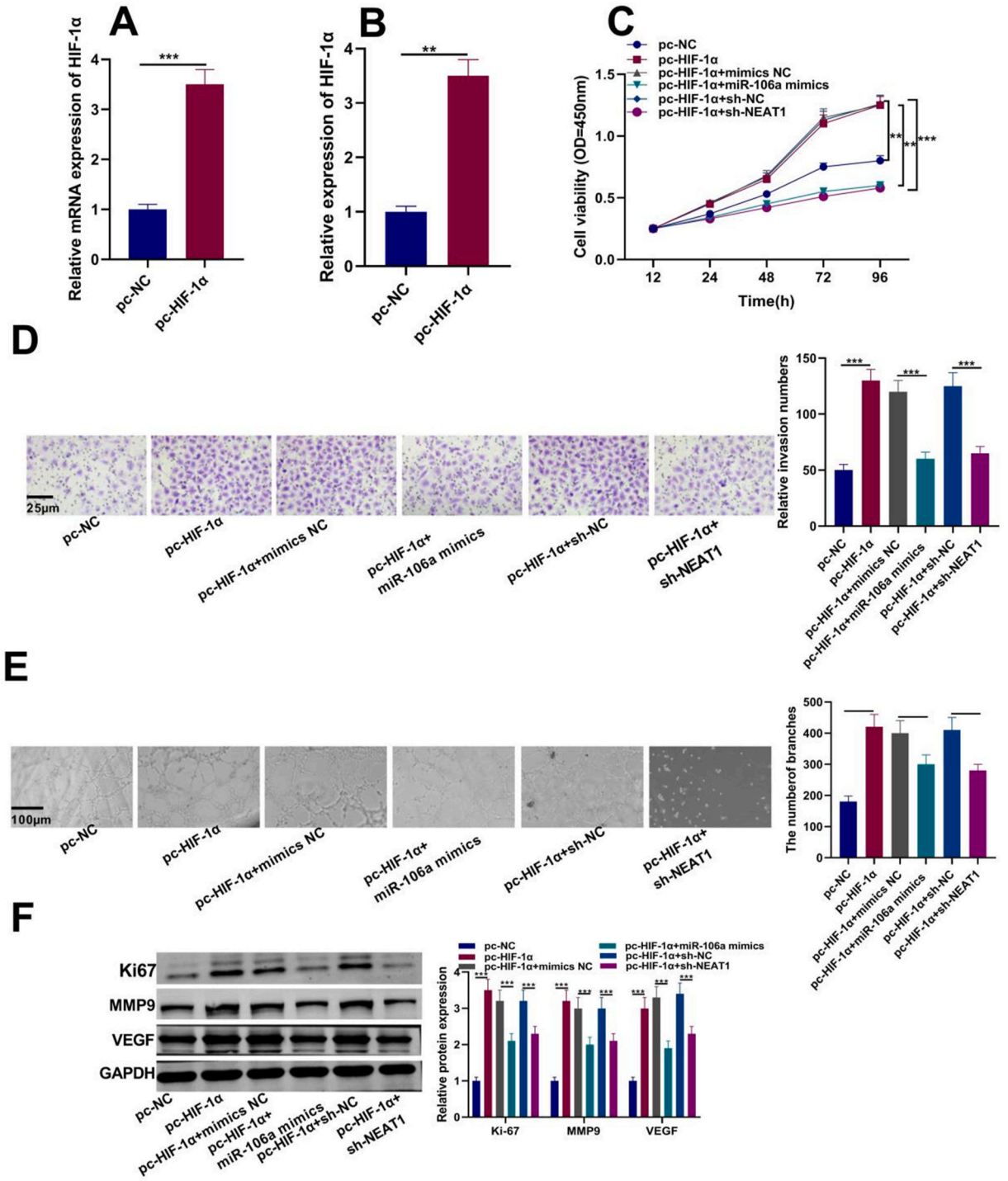

Fig. 5. NEAT1 regulates the proliferation, invasion, and tube formation of RB cells through miR-106a/HIF-1α signaling pathway. (A and B) Y-79 cells were transfected with pc-NC or pc- HIF-1α. The mRNA level (A) and protein level (B) of HIF-1α were detected by RT-qPCR and Western blotting, respectively. Y-79 cells were transfected with pc-NC, or pc-HIF-1α alone, or co-transfected with pc-HIF-1α and NC mimics, pc-HIF-1α and miR-106a mimics, pc-HIF-1α and sh-NC, pc-HIF-1α, and sh-NEAT1. (C) Cell proliferation was evaluated by the MTT assay. (D) The Transwell assay was employed to assess the invasion of pretreated Y-79 cells (magnification = 100×). (E) The capillary-like structure formation of pretreated Y-79 cells was evaluated using the tube formation assay (magnification = 100×). (F) Ki-67, MMP9, and VEGF protein levels were measured using Western blotting ((uncropped blot is available in Supplementary Fig. 5F-GAPDH, Fig. 5F-KI-67, Fig. 5F-MMP9 and Fig. 5F-VEGF).

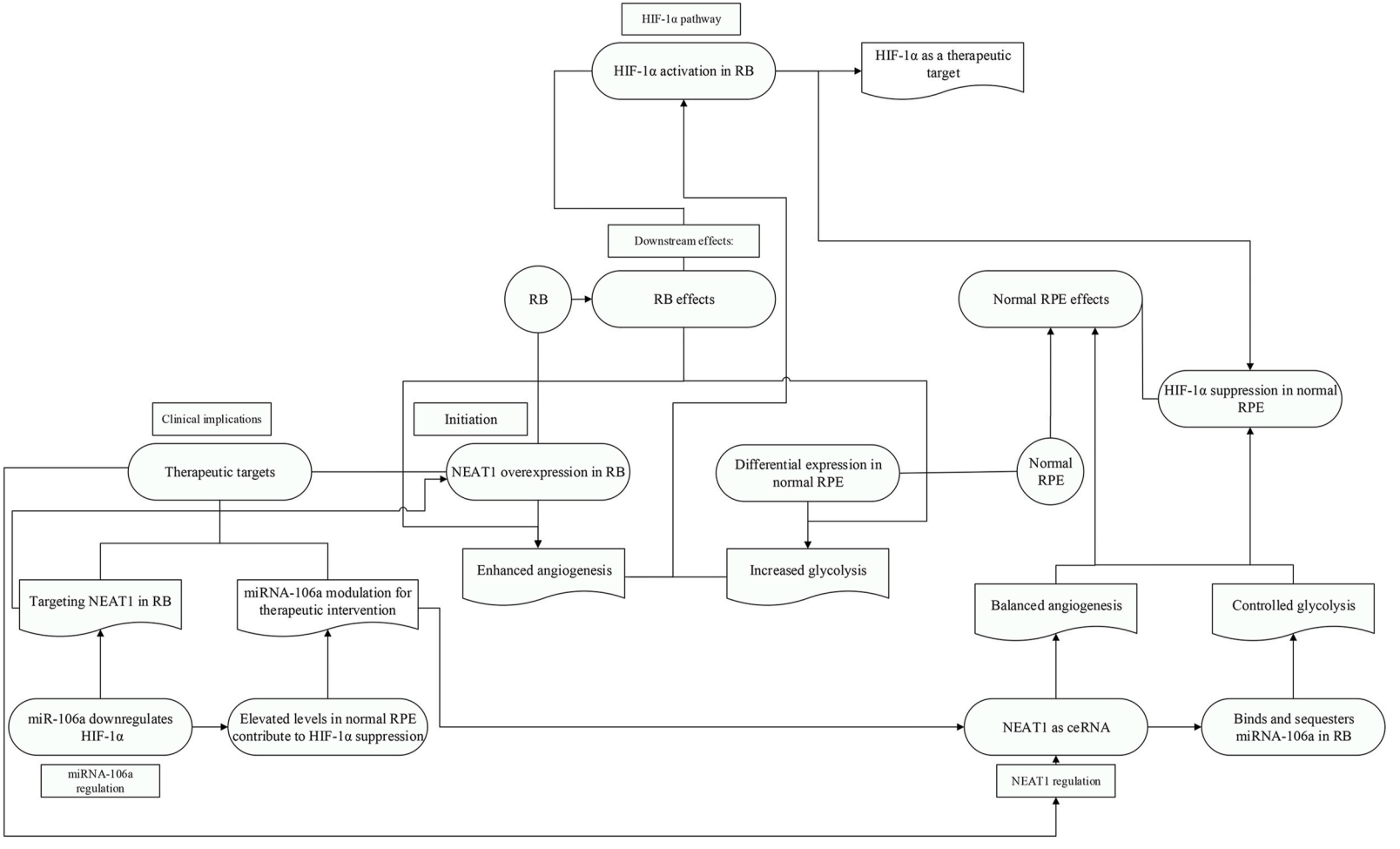

Fig. 6. The mechanism of NEAT1, miR-106a/HIF-1α in RB versus normal RPE.

5. Discussion

RB remains a major clinical challenge, accompanying by a poor prognosis in children [31]. Clarifying the molecular mechanisms underlying the occurrence and development of RB is essential to find new and effective targets for RB therapy. Recently, studies have demonstrated that lncRNAs play crucial roles in RB development and progression [24,32]. However, the functional role and underlying mechanisms of NEAT1 in RB have not yet been comprehensively explored. In the present study, it was revealed that NEAT1 expression level was upregulated in RB cells. Furthermore, it was indicated that NEAT1 could positively regulate RB cell proliferation, invasion, and angiogenesis by targeting miR-106a.

NEAT1 expression level is dysregulated in several cancer types, and it is mainly considered as an oncogene. For instance, NEAT1 expression level is elevated in breast cancer cells. Moreover, NEAT1 interference suppressed cell invasion, migration, and chemotherapy resistance [11]. Shao et al. reported that NEAT1 expression level was upregulated in cervical cancer tissues and NEAT1 knockdown inhibited the glycolysis rate of cervical cancer cells [33]. Additionally, previous studies have demonstrated that NEAT1 expression level was upregulated in RB cells compared with RPE cells, and silencing of NEAT1 repressed migration, invasion, and proliferation of RB cells, and promoted cell apoptosis [13,15]. Consistent with previously reported findings, the present study indicated that NEAT1 was enriched in Rb cells. Furthermore, NEAT1 overexpression significantly promoted RB cell proliferation, invasion, and angiogenesis of RB cells, indicating the crucial role of NEAT1 in RB cells.

Notably, lncRNAs regulate physiological processes by acting as molecular sponges for miRNAs [34]. In the present study, it was found that NEAT1 could target and positively regulate miR-106a expression level. MiR-106as a crucial tumor suppressor in diverse cancer types, including glioma, colorectal cancer, and breast cancer [35,36]. In the present study, miR-106a expression level was downregulated in RB cells compared with RPE cells, and knockdown of miR-106a increased RB cell proliferation, invasion, and angiogenesis. Furthermore, miR-106a knockdown reversed the inhibitory effects of NEAT1 silencing on RB cells. These findings suggested that NEAT1 could promote RB progression by targeting miR-106a.

HIF-1α, an important transcription factor that regulates oxygen supply and metabolic demand, is accumulated under hypoxic conditions [37]. Previous studies have shown that HIF-1α-mediated pathways are crucial to cancer progression through the regulation of cell proliferation, migration, angiogenesis, and metastasis. Consistently, the results of the present study indicated that HIF-1α expression level was higher in RB cells compared with that in RPE cells. Moreover, as a downstream target of miR-106a, HIF-1α overexpression promoted RB cell proliferation and invasion. It was recently indicated that HIF-1α could induce VEGF expression (REF), and the HIF-1α/VEGF angiogenic pathway has remarkably attracted oncologists' attention in several cancer types [37–40]. For instance, STAT1 overexpression could suppress glioma cell angiogenesis by downregulating the expression levels of HIF-1α and VEGF-A [41]. In the present study, HIF-1α overexpression induced VEGF expression level in RB cells and stimulated angiogenesis.

The present study has some limitations. Firstly, the role of the NEAT1/miR-106a/HIF-1α axis was investigated only at cellular level, while it remains elusive whether it can be validated at the animal level. Secondly, we did not collect tissues from RB patients and compared the levels of NEAT1 to normal tissue, which should be further examined in the future research. Last but not least, it remains unknown when and how to target NEAT1 to achieve an optimal treatment benefit.

6. Conclusions

In conclusion, this study revealed that increased levels of NEAT1, miR-106a, and HIF-1α could affect the progression of RB. Overexpression of NEAT1 improved the RB cell proliferation, invasion, and angiogenesis by sequestering miR-106a, leading to increase HIF-1α expression level. This study unveiled a novel underlying mechanism involving NEAT1 in RB, suggesting potential theoretical targets for the treatment of RB.

Ethics approval

The current study was approved by the Ethics Committee of the Third Medical Center of PLA General Hospital and Beijing Rehabilitation Hospital (Approval No. 2019bkkyLW007).

Funding

This study was supported by the National Natural Science Foundation of China (No. 82371051) and the Science and Technology Development Fund of Beijing Rehabilitation Hospital, Capital Medical University (No.2022-010).

Data availability statement

The datasets used and/or analyzed during the current study are available from the corresponding author upon reasonable request.

Patient consent for publication

Not applicable.

CRediT authorship contribution statement

Ying Liu: Investigation, Conceptualization. **Zhiyuan Xin:** Investigation, Conceptualization. **Kun Zhang:** Writing – original draft, Formal analysis. **Xin Jin:** Writing – review & editing, Supervision. **Dajiang Wang:** Writing – review & editing, Supervision.

Declaration of competing interest

The authors declare that they have no known competing financial interests or personal relationships that could have appeared to influence the work reported in this paper.

Acknowledgements

Not applicable.

Abbreviations

RB	Retinoblastoma
NEAT1	Nuclear enriched abundant transcript 1
HIF-1α	Hypoxia-inducible factor-1alpha
VEGF	Vascular endothelial growth factor
RT-qPCR	Quantitative reverse transcription polymerase chain reaction
lncRNAs	Long non-coding RNAs
miRNAs	MicroRNAs
RT	Room temperature
NC	Negative control

Appendix A. Supplementary data

Supplementary data to this article can be found online at https://doi.org/10.1016/j.heliyon.2024.e27653.

References

[1] A. Balmer, L. Zografos, F. Munier, Diagnosis and current management of retinoblastoma, Oncogene 25 (2006) 5341–5349.
[2] Q. Zeng, S. Wang, J. Tan, L. Chen, J. Wang, The methylation level of TFAP2A is a potential diagnostic biomarker for retinoblastoma: an analytical validation study, PeerJ 9 (2021) e10830.
[3] S.M. Imhof, A.C. Moll, A.Y. Schouten-van Meeteren, [Intraocular retinoblastoma: new therapeutic options], Ned. Tijdschr. Geneeskd. 145 (2001) 2165–2170.
[4] D.H. Abramson, C.L. Shields, F.L. Munier, G.L. Chantada, Treatment of retinoblastoma in 2015: agreement and disagreement, JAMA Ophthalmol. 133 (2015) 1341–1347.
[5] Y. Qian, L. Shi, Z. Luo, Long non-coding RNAs in cancer: implications for diagnosis, prognosis, and therapy, Front. Med. 7 (2020) 612393.
[6] M.M. Balas, A.M. Johnson, Exploring the mechanisms behind long noncoding RNAs and cancer, Noncoding RNA Res. 3 (2018) 108–117.
[7] Q. Wang, M. Gu, Y. Zhuang, J. Chen, The long noncoding RNA MAGI1-IT1 regulates the miR-302d-3p/IGF1 Axis to control gastric cancer cell proliferation, Cancer Manag. Res. 13 (2021) 2959–2967.
[8] Y. Yang, R. Wang, L. Feng, H. Ma, J. Fang, LINC00460 promotes cell proliferation, migration, invasion, and epithelial-mesenchymal transition of head and neck squamous cell carcinoma via miR-320a/BGN Axis, OncoTargets Ther. 14 (2021) 2279–2291.
[9] Y. Wang, J. Wang, H. Hao, X. Luo, lncRNA KCNQ1OT1 promotes the proliferation, migration and invasion of retinoblastoma cells by upregulating HIF-1α via sponging miR-153-3p, J. Invest. Med. 68 (2020) 1349–1356.
[10] P. Wang, Q.Y. Li, Y.N. Sun, J.T. Wang, M. Liu, Long noncoding RNA NEAT1: a potential biomarker in the progression of laryngeal squamous cell carcinoma, ORL J. Otorhinolaryngol. Relat. Spec. 83 (2021) 464–470.
[11] D. Zhou, J. Gu, Y. Wang, H. Wu, W. Cheng, Q. Wang, et al., Long non-coding RNA NEAT1 transported by extracellular vesicles contributes to breast cancer development by sponging microRNA-141-3p and regulating KLF12, Cell Biosci. 11 (2021) 68.
[12] H. Wu, A. Liu, Long non-coding RNA NEAT1 regulates ferroptosis sensitivity in non-small-cell lung cancer, J. Int. Med. Res. 49 (2021) 300060521996183.
[13] L. Luan, Q. Hu, Y. Wang, L. Lu, J. Ling, Knockdown of lncRNA NEAT1 expression inhibits cell migration, invasion and EMT by regulating the miR-24-3p/LRG1 axis in retinoblastoma cells, Exp. Ther. Med. 21 (2021) 367.
[14] W. Zhong, J. Yang, M. Li, L. Li, A. Li, Long noncoding RNA NEAT1 promotes the growth of human retinoblastoma cells via regulation of miR-204/CXCR4 axis, J. Cell. Physiol. 234 (2019) 11567–11576.
[15] L. Wang, D. Yang, R. Tian, H. Zhang, NEAT1 promotes retinoblastoma progression via modulating miR-124, J. Cell. Biochem. 120 (2019) 15585–15593.
[16] Q. Xu, L. Ye, L. Huang, L. Zhou, X. Chen, M. Ye, et al., Serum exosomal miRNA might Be a novel liquid biopsy to identify leptomeningeal metastasis in non-small cell lung cancer, OncoTargets Ther. 14 (2021) 2327–2335.
[17] B. Zheng, T. Chen, MiR-489-3p inhibits cell proliferation, migration, and invasion, and induces apoptosis, by targeting the BDNF-mediated PI3K/AKT pathway in glioblastoma, Open Life Sci. 15 (2020) 274–283.
[18] S. Dong, X. Zhang, D. Liu, Overexpression of long noncoding RNA GAS5 suppresses tumorigenesis and development of gastric cancer by sponging miR-106a-5p through the Akt/mTOR pathway, Biol. Open 8 (2019).
[19] C. Liu, Y.H. Song, Y. Mao, H.B. Wang, G. Nie, MiRNA-106a promotes breast cancer progression by regulating DAX-1, Eur. Rev. Med. Pharmacol. Sci. 23 (2019) 1574–1583.
[20] J. Lu, X. Mu, Q. Yin, K. Hu, miR-106a contributes to prostate carcinoma progression through PTEN, Oncol. Lett. 17 (2019) 1327–1332.
[21] P. Carmeliet, Y. Dor, J.M. Herbert, D. Fukumura, K. Brusselmans, M. Dewerchin, et al., Role of HIF-1alpha in hypoxia-mediated apoptosis, cell proliferation and tumour angiogenesis, Nature 394 (1998) 485–490.

[22] X. Chen, Z. Li, H. Yong, W. Wang, D. Wang, S. Chu, et al., Trim21-mediated HIF-1alpha degradation attenuates aerobic glycolysis to inhibit renal cancer tumorigenesis and metastasis, Cancer Lett. 508 (2021) 115–126.
[23] H. Liu, Z. Liang, C. Zhou, Z. Zeng, F. Wang, T. Hu, et al., Mutant KRAS triggers functional reprogramming of tumor-associated macrophages in colorectal cancer, Signal Transduct. Targeted Ther. 6 (2021) 144.
[24] X. Peng, J. Yan, F. Cheng, LncRNA TMPO-AS1 up-regulates the expression of HIF-1alpha and promotes the malignant phenotypes of retinoblastoma cells via sponging miR-199a-5p, Pathol. Res. Pract. 216 (2020) 152853.
[25] B.F. Fernandes, J. Coates, A.N. Odashiro, C. Quezada, A. Huynh, P.R. Odashiro, et al., Hypoxia-inducible factor-1alpha and its role in the proliferation of retinoblastoma cells, Pathol. Oncol. Res. 20 (2014) 557–563.
[26] Y. Liang, X. Chen, Z. Liang, MicroRNA-320 regulates autophagy in retinoblastoma by targeting hypoxia inducible factor-1alpha, Exp. Ther. Med. 14 (2017) 2367–2372.
[27] L. Zhang, L. Jin, J. Guo, K. Bao, J. Hu, Y. Zhang, et al., Chronic intermittent hypobaric hypoxia enhances bone fracture healing, Front. Endocrinol. 11 (2020) 582670.
[28] F. Yang, Z. Guo, L. Shi, Z. Li, J. Zhang, C. Chai, et al., Antiangiogenic and antitumor therapy for retinoblastoma with hypoxia-inducible factor-1α siRNA and celastrol Co-delivery nanomicelles, J. Biomed. Nanotechnol. 16 (2020) 1471–1481.
[29] D. Zhang, F.L. Lv, G.H. Wang, Effects of HIF-1alpha on diabetic retinopathy angiogenesis and VEGF expression, Eur. Rev. Med. Pharmacol. Sci. 22 (2018) 5071–5076.
[30] J. Wang, S. Wang, L. Chen, J. Tan, SCARA5 suppresses the proliferation and migration, and promotes the apoptosis of human retinoblastoma cells by inhibiting the PI3K/AKT pathway, Mol. Med. Rep. 23 (2021).
[31] T. Kivelä, The epidemiological challenge of the most frequent eye cancer: retinoblastoma, an issue of birth and death, Br. J. Ophthalmol. 93 (2009) 1129–1131.
[32] A. Wu, X. Zhou, L. Mi, J. Shen, LINC00202 promotes retinoblastoma progression by regulating cell proliferation, apoptosis, and aerobic glycolysis through miR-204-5p/HMGCR axis, Open Life Sci. 15 (2020) 437–448.
[33] X. Shao, X. Zheng, D. Ma, Y. Liu, G. Liu, Inhibition of lncRNA-NEAT1 sensitizes 5-Fu resistant cervical cancer cells through de-repressing the microRNA-34a/LDHA axis, Biosci. Rep. (2021) 41.
[34] P. Wang, S. Ning, Y. Zhang, R. Li, J. Ye, Z. Zhao, et al., Identification of lncRNA-associated competing triplets reveals global patterns and prognostic markers for cancer, Nucleic Acids Res. 43 (2015) 3478–3489.
[35] H. Zhang, Z. Ge, Z. Wang, Y. Gao, Y. Wang, X. Qu, Circular RNA RHOT1 promotes progression and inhibits ferroptosis via mir-106a-5p/STAT3 axis in breast cancer, Aging (Albany NY) 13 (2021) 8115–8126.
[36] R. Salgado-García, J. Coronel-Hernández, I. Delgado-Waldo, D. Cantú de León, V. García-Castillo, E. López-Urrutia, et al., Negative regulation of ULK1 by microRNA-106a in autophagy induced by a triple drug combination in colorectal cancer cells in vitro, Genes 12 (2021).
[37] G.L. Semenza, Hypoxia-inducible factors in physiology and medicine, Cell 148 (2012) 399–408.
[38] C. Liu, J.W. Zhang, L. Hu, Y.C. Song, L. Zhou, Y. Fan, et al., Activation of the AT1R/HIF-1 alpha/ACE axis mediates angiotensin II-induced VEGF synthesis in mesenchymal stem cells, BioMed Res. Int. 2014 (2014) 627380.
[39] A. Ahluwalia, A.S. Tarnawski, Critical role of hypoxia sensor–HIF-1alpha in VEGF gene activation. Implications for angiogenesis and tissue injury healing, Curr. Med. Chem. 19 (2012) 90–97.
[40] R.L. Jensen, B.T. Ragel, K. Whang, D. Gillespie, Inhibition of hypoxia inducible factor-1alpha (HIF-1alpha) decreases vascular endothelial growth factor (VEGF) secretion and tumor growth in malignant gliomas, J. Neuro Oncol. 78 (2006) 233–247.
[41] Y. Zhang, G. Jin, J. Zhang, R. Mi, Y. Zhou, W. Fan, et al., Overexpression of STAT1 suppresses angiogenesis under hypoxia by regulating VEGFA in human glioma cells, Biomed. Pharmacother. 104 (2018) 566–575.